



Universiteit
Leiden

The Netherlands

Multimodality Imaging of Anatomy and Function in Coronary Artery Disease

Schuijf, J.D.

Citation

Schuijf, J. D. (2007, October 18). *Multimodality Imaging of Anatomy and Function in Coronary Artery Disease*. Retrieved from <https://hdl.handle.net/1887/12423>

Version: Corrected Publisher's Version

License: [Licence agreement concerning inclusion of doctoral thesis in the Institutional Repository of the University of Leiden](#)

Downloaded from: <https://hdl.handle.net/1887/12423>

Note: To cite this publication please use the final published version (if applicable).

Chapter 11

Evaluation of Patients with Previous Coronary Stent Implantation using 64-slice Multi-Slice Computed Tomography

Joanne D. Schuijf, Gabija Pundziute, J. Wouter Jukema, Hildo J. Lamb, Joan C. Tuinenburg, Barend L. van der Hoeven, Albert de Roos, Johannes H. C. Reiber, Ernst E. van der Wall, Martin J. Schalij, Jeroen J. Bax

Abstract

Background

To prospectively evaluate the diagnostic accuracy of 64-slice Multi-Slice Computed Tomography (MSCT) for the assessment of in-stent or peri-stent restenosis, using conventional coronary angiography as the reference standard.

Methods

The study was approved by the medical ethics committee and informed consent was obtained in all 50 (40 men, mean age 60 ± 11 years) enrolled patients. In addition to conventional coronary angiography with quantitative coronary angiography (QCA), 64-slice MSCT was performed. For each stent, assessability was determined and related to stent characteristics and heart rate using Chi-Square. In the interpretable stents and peri-stent lumina (5.00mm proximal and distal to the stent), the presence of significant ($\geq 50\%$) restenosis was determined. For this analysis, partially overlapping stents were considered as a single stented segment.

Results

Of 76 stents, 65 (86%) were determined assessable. Increased heart rate and overlapping positioning were found to be associated with increased stent uninterpretability ($P < 0.05$), whereas stent location or strut thickness were not. In 7 patients stents were placed overlapping resulting in 58 stented segments available for the evaluation of significant ($\geq 50\%$) in-stent restenosis. All 6 significant ($\geq 50\%$) in-stent restenoses were detected and the absence of significant ($\geq 50\%$) restenosis was correctly identified in the 52 remaining stented segments, resulting in a sensitivity and specificity of 100%. Sensitivity and specificity for the detection of significant ($\geq 50\%$) peri-stent stenosis were 100% and 98%, respectively.

Conclusion

In selected patients with previous stent implantation, sensitivity and specificity of 100% to detect significant ($\geq 50\%$) in-stent restenosis and 100% and 98%, respectively, to detect significant ($\geq 50\%$) peri-stent stenosis were observed for 64-slice MSCT.

Introduction

Currently, follow-up imaging in patients presenting with recurrent symptoms after previous intracoronary stent placement is performed by means of conventional coronary angiography. However, this is an invasive procedure associated with a small but definite risk of serious complications^{1,2}. Considering the fact that a substantial number of procedures are not followed by an intervention, a non-invasive diagnostic procedure capable of evaluating not only native coronary arteries but also coronary stents would therefore be of great benefit.

Although promising results have been obtained using Multi-Slice Computed Tomography (MSCT) for the detection of coronary artery stenoses in native coronary arteries³⁻⁵, evaluation of metallic stents has not been as promising⁶⁻¹⁰. While substantial improvement in image quality and diagnostic accuracy was observed with 16-slice as compared to 4-slice MSCT systems, still relatively high numbers of stents with inadequate image quality were reported. In particular, stents with thicker struts or smaller diameters tended to suffer from degraded image quality^{6,7,9}.

Recently, 64-slice MSCT systems have become available and studies evaluating coronary stent assessment *in vitro* using 64-slice MSCT suggest further improvement in image quality^{11,12}. However, only limited data with 64-slice MSCT are available in patients thus far with conflicting results, as a percentage interpretable stents of 58% was recently reported by Rixe et al.¹³. Thus, the purpose of this study was to prospectively evaluate the diagnostic accuracy of 64-slice MSCT for the assessment of in-stent or peri-stent restenosis, using conventional coronary angiography as the reference standard.

Methods

Patients

The study group consisted of 50 consecutive patients (40 men, mean age 60 ± 11 years, range 41 to 79 years) who met our criteria and who had previously undergone percutaneous transluminal coronary angioplasty (PTCA) treatment in combination with stent placement. Patients were scheduled for diagnostic conventional coronary angiography from June 2005 to May 2006. In addition, MSCT coronary angiography was performed to allow non-invasive evaluation of the presence of in-stent restenosis or occlusion. Exclusion criteria were the following: 1) atrial fibrillation, 2) renal insufficiency (serum creatinine >120 mmol/L), 3) known allergy to iodine contrast media, and 4) pregnancy. All patients were on continuous beta-blocker medication, and no additional beta-blockers were administered prior to MSCT (Table 1). On average, MSCT was performed 13.4 ± 13.3 months (range 1 – 66 months) after stent implantation.

Conventional coronary angiography in combination with quantitative coronary angiography (QCA) analysis was performed on average 14 ± 9 days after MSCT and served as reference standard. All patients gave informed consent to the study protocol, which was approved by the ethics committee of the Leiden University Medical Center, after the study details, including radiation exposure, were explained.

Table 1. Clinical characteristics of the study population (n=50).

	n (%)
Gender (M/F)	40/10
Age (years)	60 ± 11
Heart Rate (bpm)	58 ± 10
Single vessel disease	22 (44%)
Multi-vessel disease	28 (56%)
Previous myocardial infarction	46 (92%)
Anterior	31 (67%)
Inferior	14 (30%)
Both	1 (2%)
Previous PTCA	50 (100%)
Previous CABG	0 (0%)
Stent location	
LM	0 (0%)
LAD	36 (47%)
LCx	11 (14%)
RCA	29 (38%)

Values are n (%).

Bpm: beats per minute; *CABG*: coronary artery bypass grafting; *LM*: Left main coronary artery; *LAD*: Left anterior descending coronary artery; *LCx*: Left circumflex coronary artery; *RCA*: Right coronary artery.

Stent characteristics

Diameter of implanted stents ranged from 2.25 to 4.0 mm with an average of 3.4 ± 0.3 mm, while stent length ranged from 8.0 mm to 33.0 mm with an average of 19.4 ± 5.0 mm. In total, 21 stents were positioned with partial overlap. Ten different stent types were evaluated, of which the majority were non-drug-eluting stents (DES): Vision (Guidant, n=33), Driver (Medtronic, n=3), Ave S7 (Medtronic, n=2), Ave S670 (Medtronic, n=1), Orbus (Orbus technologies, n=2), Tristar (Guidant, n=2), Bx Velocity (Cordis, n=1), and Liberté (Boston Scientific, n=1). In addition, 31 DES-stents (Cypher, Cordis, n=30 and Achieve, Guidant, n=1) were included.

Of these stents, Cypher, Bx Velocity and Tristar were considered to have thick struts (≥ 140 μm).

Data acquisition

Multi-Slice Computed Tomography

MSCT was performed using a Toshiba Multi-slice Aquilion 64 system (Toshiba Medical Systems, Tokyo, Japan) with a collimation of 64 x 0.5 mm and a rotation time of 0.4, 0.45 or 0.5 s, depending on the heart rate. The tube current was 350 mA, at 120 kV. Non-ionic contrast material was administered in the antecubital vein with an amount of 90-105 ml, depending on the total scan time, and a flow rate of 5.0 ml/sec (Iomeron 400[®]). Repetitive low-dose monitoring examinations (120 kV, 10 mA) were performed 5 seconds after the start of contrast medium injection. After the preset contrast enhancement threshold level of baseline HU + 100 HU in the descending aorta was reached, the MSCT

examination was automatically initiated. After a 2 second delay, data acquisition was performed during an inspiratory breath hold of approximately 10 seconds, while the ECG was recorded simultaneously to allow retrospective gating of the data.

For evaluation of the coronary arteries and intracoronary stents, data were reconstructed using a segmented reconstruction algorithm at 75% of the R-R interval with a slice thickness of 0.5 mm and a reconstruction interval of 0.3 mm. If motion artefacts were still present in this phase, additional reconstructions were explored to obtain the reconstruction phase with least motion artefacts (23 patients). For this purpose, images were reconstructed at a single level throughout the R-R interval in steps of 20ms to obtain information on the individual patient's pattern of cardiac motion. Based on these images, the time point to reconstruct the entire data set was chosen. Also, in all patients, an additional data set was reconstructed in the most optimal phase(s) using a sharper reconstruction kernel (Q04 instead of Q05-07) to improve stent image quality¹⁴. MSCT was performed successfully in all patients. Average heart rate during the acquisition was 58 ± 10 (range 38 to 86).

Conventional coronary angiography

Conventional coronary angiography was performed according to standard techniques by 2 experienced operators with respectively 10 and 15 years experience. Vascular access was obtained using the femoral approach with the Seldinger technique and a 6-French catheter.

Data analysis

Multi-Slice Computed Tomography

For each individual coronary artery, the data set containing no or the least motion artifacts was transferred to a dedicated workstation (Vitrea2, Vital Images, Plymouth, Minn. USA) for post-processing. Coronary stents were evaluated on both the standard kernel and sharper kernel reconstructions using predominantly the original axial MSCT images, while manually obtained curved multiplanar reconstructions were used for verification of findings. 3D volume rendered reconstructions were not used. In addition, the axial images and curved multiplanar reconstructions were viewed in 3 different window and level settings; 1000/200 HU as a standard window level while also window levels of 1600/300 HU and 2500/900 HU were used to improve stent appearance. Assessment was performed blinded to the conventional coronary angiography results in consensus reading by 2 experienced observers, both having 3.5 years experience in the evaluation of MSCT coronary angiography, with one also having extensive (15 years) experience in conventional coronary angiography and intervention.

First, each individual stent was assigned an image quality score of: 1 (good image quality, no artifacts), 2 (moderate image quality, minor or moderate artifacts present but diagnosis possible) or 3 (uninterpretable, no diagnosis possible) as previously described^{9,15}. Also, it was documented whether stents were positioned partially overlapping or not. If so, the stents were consequently considered as a single stented segment for the evaluation of in-stent or peri-stent stenosis.

Subsequently, the presence of significant restenosis ($\geq 50\%$ reduction of lumen diameter) was as-

essed for each stented segment, while also the observation of non-significant (<50% reduction of lumen diameter) neo-intima hyperplasia within the stented segment was documented. Finally, since restenosis of the stent borders may also regularly occur, the presence of peri-stent stenosis, $\geq 50\%$ narrowing of luminal diameter 5.00 mm proximal and distal to the stented segment was also evaluated as previously described ⁹.

Conventional and quantitative coronary angiography

Conventional angiograms were evaluated in consensus by two experienced observers without knowledge of the MSCT data. First, the location of the intracoronary stents was identified on the images before contrast injection. Subsequently, QCA with automated vessel contour detection after catheter-based image calibration was performed in end-diastolic frames by 2 qualified observers with respectively 2 and 10 years experience in QCA using a standard algorithm dedicated for stent analysis (Brachy-DES analysis, QCA-CMS version 6.0, Medis, Leiden, The Netherlands) ¹⁶. QCA was performed of the stented segment as well as its proximal and distal (5.00 mm) lumina and percentage diameter reduction was determined. An in-stent lumen diameter narrowing $\geq 50\%$ in diameter (up to in-stent occlusion) was defined as a significant restenosis.

Statistical analysis

Continuous variables are presented as means \pm one standard deviation (SD), whereas categorical data are summarized as frequencies and percentages. In order to relate stent assessability to stent characteristics, stents were divided according to location in the coronary tree and according to strut thickness (with stents with $\geq 140 \mu\text{m}$ struts regarded as having thick struts and stents with $< 140 \mu\text{m}$ struts regarded as having thin struts), as previously described ⁹. Distinction was also being made between stents positioned partially overlapping or not. Percentage assessable stents was calculated for each category and compared using Chi-Square analysis with Yates' correction. In addition, average heart rate was compared between interpretable stents and stents uninterpretable due to attenuation artefacts or motion artefacts using the Student's *t* test for independent samples. Logistic regression analyses were applied to correlate segment and patient characteristics to image quality, using the generalized estimating equation (GEE) method developed by Liang and Zeger ¹⁷. Two (dichotomous) outcome variables were considered: good versus moderate-or-uninterpretable image quality, and good-or-moderate quality versus uninterpretable image quality. The GEE analyses were performed with proc GENMOD with a binominal distribution for the outcome variable, the link function specified as logit, and patients as separate subjects. Odds ratios and 95% confidence intervals (CI) are reported. Sensitivity, specificity, positive and negative predictive values (including 95% confidence intervals) for the detection of in-stent restenosis $\geq 50\%$, as determined by conventional angiography in combination with QCA, were determined for each stented segment. In addition, diagnostic accuracy was also determined for the detection of significant ($\geq 50\%$) narrowing of the peri-stent lumina (5.00 mm proximal and distal to the stented segment).

Table 2. Results from GEE analysis

	Odds Ratio (95% CI)
Good versus moderate-or-uninterpretable image quality	
Heart rate*	0.98 (0.93-1.05)
Overlapping (Y/N)	0.70 (0.17-2.96)
Strut Thickness ($\geq 140\mu\text{m}$ or $< 140\mu\text{m}$)	0.44 (0.15-1.29)
Good-or-moderate versus uninterpretable image quality	
Heart rate*	0.94 (0.86-1.03)
Overlapping (Y/N)	0.16 (0.03-0.87)
Strut Thickness ($\geq 140\mu\text{m}$ or $< 140\mu\text{m}$)	0.38 (0.08-1.77)

* Odds ratio per beat per minute

Abbreviations: CI: confidence interval

Statistical analyses were performed using SPSS software (version 12.0, SPSS Inc, Chicago, IL, USA) and SAS software (The SAS system, release 6.12, Cary, NC, USA: SAS Institute Inc.). A value of $P < 0.05$ was considered statistically significant.

Results

Stent analysis; image quality

The 50 patients had a total of 76 stents (1 to 5 stents per patient, average 1.5 ± 0.87) that were studied. A total 41 (54%) and 24 (32%) stents were of respectively good or moderate image quality, whereas stent lumen could not be visualized in the remaining 11 (14%) stents. Reasons of uninterpretability were motion artifacts in 5 (45%) stents and attenuation artefacts in 6 (55%) stents.

Of the uninterpretable stents, 6 were placed in the right coronary artery (RCA), whereas 3 and 2 were positioned in the left anterior descending (LAD) and left circumflex coronary arteries (LCx), respectively. No significant differences were observed in interpretability between the different coronary arteries ($P=0.35$).

Average heart rate during data acquisition was significantly higher in stents deemed uninterpretable due to motion artifacts (72 ± 9) as compared to stents deemed uninterpretable due to attenuation artefacts (55 ± 2 , $P=0.002$). No significant difference was observed between stents uninterpretable due to attenuation artefacts and interpretable stents (57 ± 9 , $P=0.62$).

In stents positioned without any overlap ($n=55$), image quality was good in 31 (56%), moderate in 20 (36%) and non-diagnostic in 4 (7%). In contrast, image quality in stents positioned with partial overlap ($n=21$) was significantly lower as image quality in these stents was good in 10 (48%) and moderate in 4 (19%), whereas 7 (33%) were uninterpretable ($P=0.01$).

A trend towards improved image quality in stents with thin struts ($< 140 \mu\text{m}$; $n=43$) could be observed as compared to stents with thick struts ($\geq 140 \mu\text{m}$; $n=33$). In the latter 14 (42%) and 12 (36%) were of respectively good or moderate image quality with 7 (21%) stents being uninterpretable.

In contrast, respectively 27 (63%) and 12 (28%) of stents with thinner struts were of either good or moderate image quality, while 4 (9%) stents were uninterpretable. Still, no statistical significance was observed ($P=0.15$).

Results from GEE analyses are provided in Table 2.

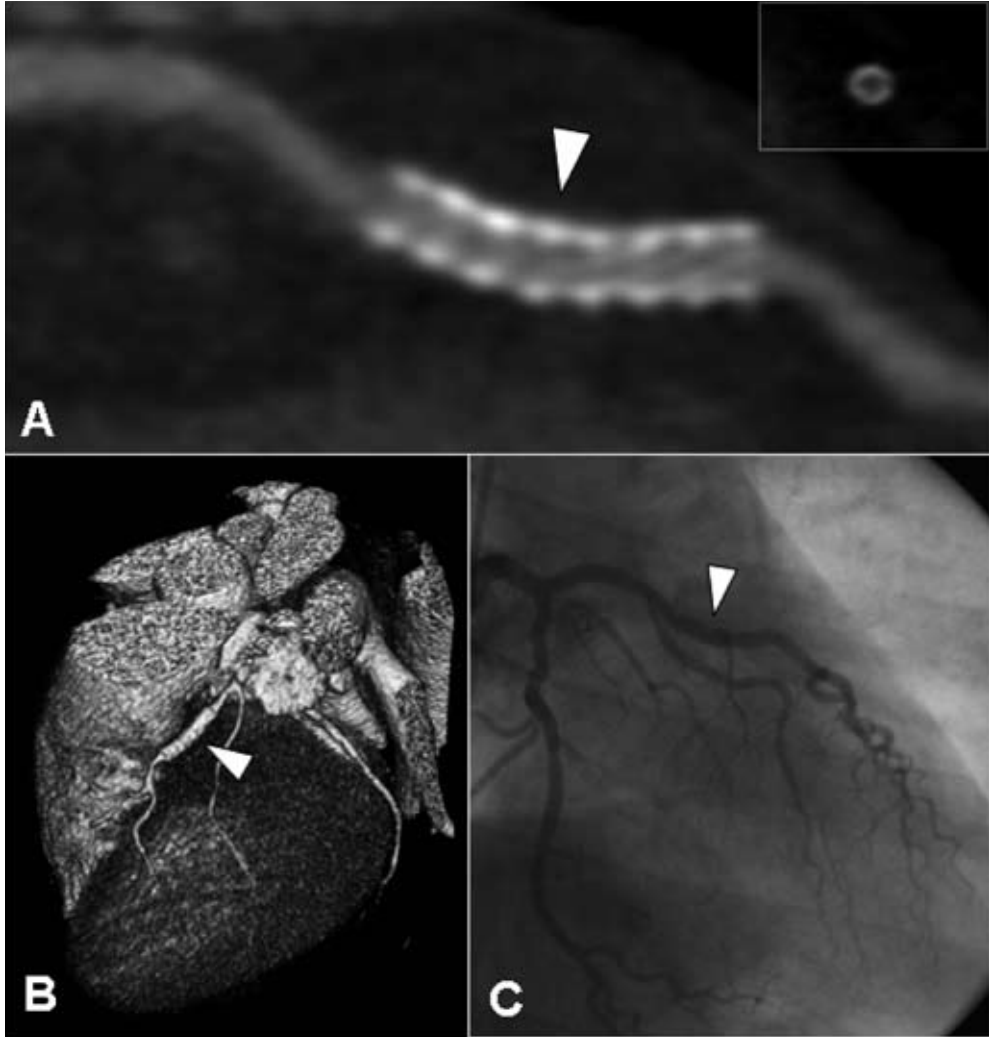


Figure 1. Example of a patent thick-strut drug-eluting stent (diameter 3.5 mm) placed in the left anterior descending coronary artery of a 53-year old male patient. In Panels A and B, a curved multiplanar and 3D volume rendered reconstruction are provided, showing a patent thick-strut drug-eluting stent with only limited neo-intima hyperplasia (white arrowhead). Also on the cross-sectional image (insert Panel A), no significant in-stent restenosis can be observed. The corresponding conventional coronary angiogram is provided in Panel C.

Stent analysis; diagnosis of (significant) in-stent restenosis (Table 3)

In 7 patients, a total of 21 stents were placed partially overlapping, thereby hampering individual evaluation of the presence of in-stent restenosis. Consequently, overlapping stents were considered as a single stented segment, resulting in the availability of 58 stented segments for the diagnosis of significant ($\geq 50\%$ of lumen diameter reduction) in-stent restenosis. Significant restenosis was correctly ruled out in all 52 stented segments without significant in-stent restenosis as determined by conventional coronary angiography in combination with QCA (Figures 1 and 2). The remaining 6 stented segments with significant in-stent restenosis were correctly identified on MSCT (Figure 3). Accordingly, the sensitivity and specificity for the assessment of significant in-stent restenosis were 100%. In the 52 stented segments without significant in-stent restenosis, average luminal narrowing as determined by QCA was $23.4 \pm 8.6\%$ (range: 4.3% to 42.4%). Non-significant restenosis could be observed on MSCT in 37 (71%) stented segments, whereas no neo-intima hyperplasia could be observed on MSCT in 15 stented segments. In stented segments without neo-intima hyperplasia visible on MSCT, average luminal narrowing as determined by QCA was slightly but not significantly lower as compared to that of stented segments with visible neo-intima hyperplasia ($20.6\% \pm 11.7\%$ vs. $24.0\% \pm 7.6\%$).

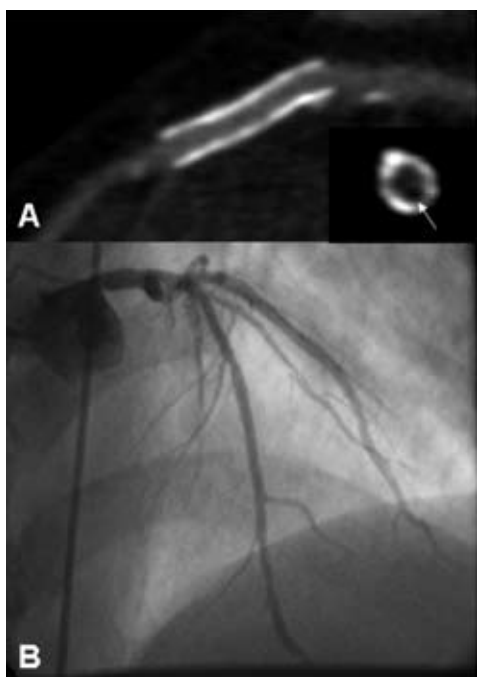


Figure 2. Example of a patent thin-strut, non-drug-eluting stent placed in the left anterior descending coronary artery of a 46-year old male patient. In Panel A, a curved multiplanar reconstruction is provided of a patent thin-strut stent (diameter 3.5 mm). Cross-sectional image perpendicular of the stent (insert) confirms the presence of only minimal in-stent hyperplasia (appearing as a small rim of hypoattenuating tissue, white arrow). Observations were confirmed by invasive coronary angiography (Panel B).

Peri-stent lumina (Table 3)

Of the 76 implanted stents, 21 were positioned (partially) overlapping. As a result, 55 single stented segments and 10 stented segments resulting from overlapping stents were available, including both interpretable as uninterpretable stented segments. Also, 1 stent (located in the RCA) originated directly from the aorta. Accordingly, 64 proximal stent lumina and 65 distal stent lumina were available for analysis. All but 1 (1%) of the 129 peri-stent lumina were of sufficient image quality to evaluate the presence of significant narrowing. Conventional coronary angiography in combination with QCA demonstrated the presence of significant stenosis of 5 peri-stent lumina, which were all correctly identified on MSCT. However, 2 lesions (1 proximal and 1 distal) were overestimated by MSCT, resulting in a specificity of 98%.

Table 3. Diagnostic accuracy to detect (significant) in-stent or peri-stent restenosis.

	≥ 50% in-stent restenosis	Peri-stent restenosis
Assessable*	65/76 (86%, 78% - 94%)	128/129 (99%, 97% - 100%)
Sensitivity	6/6 (100%)	5/5 (100%)
Specificity	52/52 (100%)	121/123 (98%, 96% - 100%)
Positive predictive value	6/6 (100%)	5/7 (71%, 37% - 100)
Negative predictive value	52/52 (100%)	121/121 (100%)

Values are segments (%; 95% confidence intervals).

* Includes all available stents, for the diagnostic accuracy calculations, (partially) overlapping positioned stents were considered as a single stented segment.

Discussion

In our present study, 76 coronary stents were evaluated using 64-slice MSCT, of which 65 (86%) were interpretable. Both elevated heart rate and overlapping positioning appeared to be associated with decreased interpretability, while no effect of stent type or location was observed. In the interpretable stented segments, a sensitivity and specificity to detect significant ($\geq 50\%$) in-stent restenosis of 100% was obtained, whereas the presence of non-obstructing in-stent restenosis was accurately identified in 71% of stented segments. Also the presence of peri-stent stenosis could be accurately detected with a sensitivity and specificity of 100% and 98%, respectively.

Our current observations compare favourably to previous studies reporting on coronary stent imaging with 16-slice MSCT. In an earlier study by Schuijff et al, 21 patients with 65 previously implanted stents were evaluated⁹. A moderate sensitivity 78% and an excellent specificity of 100%, respectively, to detect in-stent restenosis were observed. However, only 50 (77%) of stents proved to be of sufficient image quality for evaluation. Exploration of the characteristics of 23% uninterpretable stents showed that predominantly stents with thicker struts ($\geq 140 \mu\text{m}$) as well as stents with smaller diameter (e.g. $\leq 3.0 \text{ mm}$) tended to suffer from degraded image quality. The effect of thick struts was particularly pronounced, 41% of thick strut stents were uninterpretable, as compared to 11% of stents with thinner struts. Diameter showed less prominent effect, although still a substantially

higher percentage of stents with a diameter ≤ 3.0 mm was uninterpretable as compared to stents with a larger diameter (28% versus 11%). These observations were recently confirmed in a larger population (143 patients included with a total of 232 stents)⁶. In this study by Gilard et al, also using 16-slice MSCT, a substantial increase in interpretability from 51% to 81% was observed in stents with diameters > 3.0 mm as compared to those with diameters ≤ 3.0 mm. In addition, sensitivity to detect in-stent restenosis increased similarly from 54% to 86%. For all stents, regardless of diameter, a specificity of 100% was observed. In this particular study the effect of strut thickness was not explored.

In our present study, improved interpretability of stents with 64-slice MSCT was observed with sufficient image quality in 86% of stents. Exploration of the characteristics of uninterpretable stents showed that similar to previous studies in native coronary arteries, elevated heart rate was a significant cause of non-diagnostic image quality¹⁸. Indeed, uninterpretability was due to motion artefacts in 45% of uninterpretable stents. Accordingly, these observations underline the need for adequate heart rate control during MSCT coronary angiography.

Further evaluation of the uninterpretable stents demonstrated that also partially overlapping positioned stents are associated with deteriorated image quality. The increased metal content is likely to amplify high-density artefacts, thereby increasing the artificial narrowing of the stent lumen. Indeed, whereas 93% of single stents were interpretable, 33% of partially overlapping stents were of non-diagnostic quality. Accordingly, in patients with partially overlapping stents, evaluation by means of another modality than MSCT may be preferred. In contrast to previous studies, no pronounced effect of strut thickness was observed. Nonetheless, the presence of thick struts still tended to result in non-diagnostic image quality more often as compared to stents with thin struts (21% versus 9%, $P=0.15$). Accordingly, the influence of strut thickness on image quality with 64-slice MSCT should be evaluated in larger cohort as our study may have been underpowered to demonstrate any effect.

In the interpretable stented segments, the presence or absence of significant ($\geq 50\%$) in-stent restenosis was correctly identified in all stented segments. Also, the presence or absence of peri-stent restenosis could be detected with diagnostic accuracy of 98%. In particular, observed negative predictive value to exclude the presence of in-stent or peri-stent restenosis was extremely high. Accordingly, the technique may be well suited for non-invasive rule out of significant ($\geq 50\%$) in-stent or peri-stent restenosis. Somewhat lower sensitivity and specificity were reported by a recent study employing 40-slice MSCT technology¹⁹. In this study by Gaspar and colleagues, evaluating 65 patients with 111 implanted coronary stents, a sensitivity and specificity to detect $\geq 50\%$ in-stent restenosis of 89% and 81% were observed¹⁹. In part, this discrepancy may be explained by the fact that in this study only a very small number of stents (5%) were excluded from the analysis, whereas the number of excluded stents was higher in our own study. Still, also in the study by Gaspar, a high negative predictive value (97%) was observed, underlining the potential of MSCT as a non-invasive technique to rule out the presence of in-stent restenosis.

Another finding of our study was that in contrast to 16-slice MSCT^{9,14} the superior image quality of 64-slice MSCT has improved visualization of non-significant in-stent hyperplasia in addition to significant in-stent restenosis. The presence of in-stent hyperplasia albeit limited was demonstrated

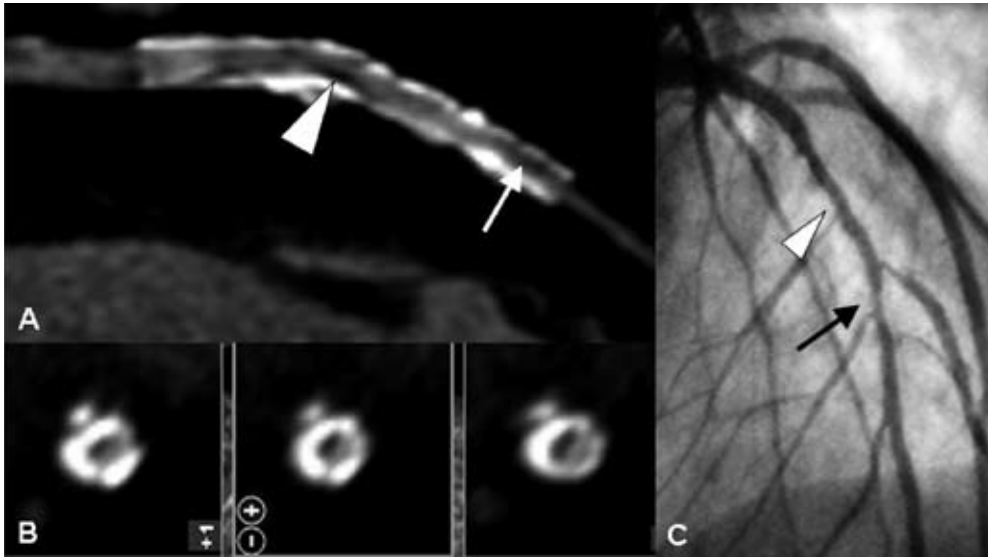


Figure 3. Diagnosis of in-stent restenosis in 2 adjacent stents placed in the left anterior descending coronary artery of a 61-year old male patient. Curved multiplanar reconstruction (Panel A) demonstrates the presence of in-stent restenosis (slightly exceeding 50% luminal diameter narrowing at the mid level [white arrowhead] and more severe at the distal part of the stent [white arrow]) in 2 adjacent non-drug-eluting stents (diameter 3.5 and 3.0 mm). Panel B: Also on the cross-sectional images obtained at the mid level, the presence of in-stent restenosis (appearing as hypoattenuating tissue) can be observed. Panel C: Findings were confirmed by invasive coronary angiography.

by QCA in all stents and correctly recognized in 71% of stents on MSCT as well. Our observations are in line with a recent study by Mahnken et al using 64-slice MSCT in a phantom model²⁰. Comparison of 16-slice MSCT to 64-slice MSCT in 8 stents with a diameter of 3.0 mm positioned in a static chest phantom showed superior visualization of stent lumina with 64-slice MSCT due to significantly less artificial lumen reduction and image noise. Still, a considerable portion of stent lumina remained obscured even with 64-slice MSCT and in our own study, the presence of neo-intima hyperplasia could not be observed on MSCT in 30% of stents. Accordingly, the value of MSCT to identify moderate in-stent hyperplasia appears to remain limited at present.

Limitations

A relatively small number of patients were evaluated in the present study. As a result, the total number of stents and importantly, the number of patients with significant in-stent restenosis (12%), were relatively low as well. Nonetheless, a much higher prevalence of in-stent restenosis is not likely to be encountered in daily practice and extrapolation of the current results to clinical practice may therefore be justifiable^{21;22}. Also, the number of evaluated stents was low and the influence of stent and patient characteristics on stent interpretability should be explored in larger patient cohorts in order

to fully establish which characteristics should potentially be avoided when performing stent evaluation with MSCT. In particular, the range of stent diameters was limited in the present study with an average of 3.4 ± 0.3 mm and as a result a potential effect of stent diameter could not be evaluated in the present study. Thus, our study could possibly best be regarded as a basis for further larger studies concerning image quality and diagnostic accuracy of 64-slice MSCT in coronary stents. In addition, despite the technological advancements of 64-slice MSCT, several limitations inherent to the technique remain. First, as also observed in our present study, a stable and low heart rate remains crucial for high-quality MSCT images and administration of beta-blockers prior to the examination therefore is often required¹⁸. Finally, an important consideration is the relatively high effective radiation dose (10-15 mSv) to which a patient undergoing MSCT coronary angiography is exposed. For this purpose, dose-modulation protocols are currently under development.

Conclusion

In selected patients with previous stent implantation, sensitivity and specificity of 100% to detect significant ($\geq 50\%$) in-stent restenosis and 100% and 98%, respectively, to detect significant ($\geq 50\%$) peri-stent stenosis were observed for 64-slice MSCT. In particular, the technique may be useful for non-invasive exclusion of in-stent or peri-stent restenosis and avoid invasive imaging in a considerable number of patients.

References

1. Krone RJ, Johnson L, Noto T. Five year trends in cardiac catheterization: a report from the Registry of the Society for Cardiac Angiography and Interventions. *Cathet Cardiovasc Diagn.* 1996;39:31-35.
2. Scanlon PJ, Faxon DP, Audet AM, Carabello B, Dehmer GJ, Eagle KA, Legako RD, Leon DF, Murray JA, Nissen SE, Pepine CJ, Watson RM, Ritchie JL, Gibbons RJ, Cheitlin MD, Gardner TJ, Garson A, Jr., Russell RO, Jr., Ryan TJ, Smith SC, Jr. ACC/AHA guidelines for coronary angiography. A report of the American College of Cardiology/American Heart Association Task Force on practice guidelines (Committee on Coronary Angiography). Developed in collaboration with the Society for Cardiac Angiography and Interventions. *J Am Coll Cardiol.* 1999;33:1756-1824.
3. Achenbach S, Giesler T, Ropers D, Ulzheimer S, Derlien H, Schulte C, Wenkel E, Moshage W, Bautz W, Daniel WG, Kalender WA, Baum U. Detection of coronary artery stenoses by contrast-enhanced, retrospectively electrocardiographically-gated, multislice spiral computed tomography. *Circulation.* 2001;103:2535-2538.
4. Nieman K, Rensing BJ, van Geuns RJ, Munne A, Ligthart JM, Pattynama PM, Krestin GP, Serruys PW, de Feyter PJ. Usefulness of multislice computed tomography for detecting obstructive coronary artery disease. *Am J Cardiol.* 2002;89:913-918.
5. Mollet NR, Cademartiri F, van Mieghem CA, Runza G, McFadden EP, Baks T, Serruys PW, Krestin GP, de Feyter PJ. High-resolution spiral computed tomography coronary angiography in patients referred for diagnostic conventional coronary angiography. *Circulation.* 2005;112:2318-2323.
6. Gilard M, Cornily JC, Pennec PY, Le Gal G, Nonent M, Mansourati J, Blanc JJ, Boschhat J. Assessment of coronary artery stents by 16 slice computed tomography. *Heart.* 2006;92:58-61.
7. Kitagawa T, Fujii T, Tomohiro Y, Maeda K, Kobayashi M, Kunita E, Sekiguchi Y. Noninvasive assessment of coronary stents in patients by 16-slice computed tomography. *Int J Cardiol.* 2005.
8. Kruger S, Mahnken AH, Sinha AM, Borghans A, Dedden K, Hoffmann R, Hanrath P. Multislice spiral computed tomography for the detection of coronary stent restenosis and patency. *Int J Cardiol.* 2003;89:167-172.
9. Schuijf JD, Bax JJ, Jukema JW, Lamb HJ, Warda HM, Vliegen HW, de Roos A, van der Wall EE. Feasibility of assessment of coronary stent patency using 16-slice computed tomography. *Am J Cardiol.* 2004;94:427-430.
10. Cademartiri F, Marano R, Runza G, Mollet N, Nieman K, Luccichenti G, Gualerzi M, Brambilla L, Coruzzi P, Galia M, Midiri M. Non-invasive assessment of coronary artery stent patency with multislice CT: preliminary experience. *Radiol Med (Torino).* 2005;109:500-507.
11. Maintz D, Seifarth H, Raupach R, Flohr T, Rink M, Sommer T, Ozgun M, Heindel W, Fischbach R. 64-slice multidetector coronary CT angiography: in vitro evaluation of 68 different stents. *Eur Radiol.* 2005;1-9.
12. Seifarth H, Ozgun M, Raupach R, Flohr T, Heindel W, Fischbach R, Maintz D. 64- Versus 16-slice CT angiography for coronary artery stent assessment: in vitro experience. *Invest Radiol.* 2006;41:22-27.
13. Rixe J, Achenbach S, Ropers D, Baum U, Kuettner A, Ropers U, Bautz W, Daniel WG, Anders K. Assessment of coronary artery stent restenosis by 64-slice multi-detector computed tomography. *Eur Heart J.* 2006;27:2567-2572.
14. Hong C, Chrysant GS, Woodard PK, Bae KT. Coronary artery stent patency assessed with in-stent contrast enhancement measured at multi-detector row CT angiography: initial experience. *Radiology.* 2004;233:286-291.
15. Watanabe M, Uemura S, Iwama H, Okayama S, Takeda Y, Kawata H, Horii M, Nakajima T, Hirohashi S, Kichikawa K, Ookura A, Saito Y. Usefulness of 16-slice multislice spiral computed tomography for follow-up study of coronary stent implantation. *Circ J.* 2006;70:691-697.
16. Reiber JH, Serruys PW, Kooijman CJ, Wijns W, Slager CJ, Gerbrands JJ, Schuurbiens JC, den Boer A, Hugenholtz PG. Assessment of short-, medium-, and long-term variations in arterial dimensions from computer-assisted quantitation of coronary cineangiograms. *Circulation.* 1985;71:280-288.
17. Liang KY, Zeger SL. Longitudinal Data-Analysis Using Generalized Linear-Models. *Biometrika.* 1986;73:13-22.
18. Cademartiri F, Mollet NR, Runza G, Belgrano M, Malagutti P, Meijboom BW, Midiri M, Feyter PJ, Krestin GP. Diagnostic accuracy of multislice computed tomography coronary angiography is improved at low heart rates. *Int J Cardiovasc Imaging.* 2005;1-5.

19. Gaspar T, Halon DA, Lewis BS, Adawi S, Schliamser JE, Rubinshtein R, Flugelman MY, Peled N. Diagnosis of coronary in-stent restenosis with multidetector row spiral computed tomography. *J Am Coll Cardiol.* 2005;46:1573-1579.
20. Mahnken AH, Muhlenbruch G, Seyfarth T, Flohr T, Stanzel S, Wildberger JE, Gunther RW, Kuettner A. 64-slice computed tomography assessment of coronary artery stents: a phantom study. *Acta Radiol.* 2006;47:36-42.
21. Moses JW, Leon MB, Popma JJ, Fitzgerald PJ, Holmes DR, O'Shaughnessy C, Caputo RP, Kereiakes DJ, Williams DO, Teirstein PS, Jaeger JL, Kuntz RE. Sirolimus-eluting stents versus standard stents in patients with stenosis in a native coronary artery. *N Engl J Med.* 2003;349:1315-1323.
22. Gordon PC, Gibson CM, Cohen DJ, Carrozza JP, Kuntz RE, Baim DS. Mechanisms of restenosis and redilation within coronary stents-- quantitative angiographic assessment. *J Am Coll Cardiol.* 1993;21:1166-1174.

